Bulletin du Service Géologique de l'Algérie
Vol. **30**, n° **1**, pp.**113-130**, **9** fig. **2021**

IMPACT OF THE COMPACTION HISTORY ON THE PETROPHYSICAL AND THERMAL PROPERTIES OF THE TIMIMOUN-AHNET BASIN: INSIGHTS INTO THE HYDROCARBON SYSTEM IN THE REGION

Lubna AMIR*, Rachid AIT OUALI*,[1], Ahmed NEDJARI*, Nabila OUBACHA* and Belkacem HELLAL*

ABSTRACT

Here, we investigate the role of the compaction for oil and gas generation in the Timimoun-Ahnet basin (Sahara, Southwest of Algeria). Firstly, a well logging analysis was carried out for seven boreholes in the region and helped to provide with the input data necessary for basin modeling with the TherMO'S software. Petrophysical and thermal properties for source rocks' levels and reservoirs were then simulated considering the burial history all through the calculations. The study highlights three main burial phases for source rocks and reservoirs deposits. The results obtained also revealed that the conditions provided to the organic matter were sufficient to propose the beginning of hydrocarbons generation prior to the Hercynian event. Oil and gas cracking were also favored by the Late Triassic thermal event.

Keywords - Timimoun - Basin Modeling - Burial - Petrophysics - Thermal - Oil - Gas.

INFLUENCE DE LA COMPACTION DANS L'ÉVOLUTION DES PARAMÈTRES PÉTROPHYSIQUES ET THERMIQUES DU BASSIN DE TIMIMOUN-AHNET : CONTRIBUTION À LA COMPRÉHENSION DU SYSTÈME PÉTROLIER DANS LA RÉGION

RÉSUMÉ

Dans cette étude, nous avons mis en évidence le rôle de la compaction et de la variation des taux d'enfouissement au cours de l'histoire du bassin de Timimoun pour expliquer les conditions qui ont favorisé la genèse des hydrocarbures. Nous avons ainsi analysé les enregistrements diagraphiques de sept sondages afin d'alimenter un modèle numérique intégrant la variation du gradient thermique au cours de l'histoire des bassins sédimentaires. Les résultats ont permis de retrouver trois phases principales d'enfouissement des séries mères (Silurien, Frasnien) et réservoirs, et de suggérer l'occurrence d'évènements thermiques régionaux (Trias) ayant influencé l'évolution des paramètres pétrophysiques et thermiques du bassin.

Mots-clés - Timimoun - Simulation Numérique - Enfouissement - Pétrophysique - Thermique - Huile - Gaz.

*Faculté des Sciences de la Terre, Géographie et Aménagement du Territoire (FSTGAT), USTHB, BP 32, 16111, El Alia, Bab Ezzouar, Alger, Algerie. E-mails: lamir@usthb.dz; nedjaria@gmail.com; o_nabila@hotmail.com; belkacem.hellal@live.fr.
[1] Décédé en 2020.

- Manuscrit déposé le 02 fevrier 2020, accepté après révision le 19 avril 2020.

I- INTRODUCTION

In Algeria, the Saharan Domain (North Africa) is the location for oil and gas resources. In fact, the progressive segmentation of the Northern Gondwana shelf into intracratonic basins and swells was mainly a consequence of the Upper Devonian to Upper Carboniferous collision of the Northern Gondwana with the Laurasia (Lüning *et al.,* 2000). Figure 1a shows the oil and gas deposit reported by Askri *et al.* (1995) in the country. It appears that the South-western is dominated by gas resources. In fact, located in Southwestern part of Algeria, the Ahnet - Timimoun basin contains the most important reserves of gas discovered to date in Algeria (Drid *et al.,* 1998). The complexity of the Timimoun basin results from a geodynamic context related to its position at the junction between two different intracratonic shields (Nedjari *et al.,* 2009; Nedjari and Ait Ouali, 2018). Several authors investigated through geochemistry analysis the reason gas resources dominate in the region to the detriment of oil (Drid *et al.,* 1998; Kadi *et al.,* 2013). Previous reports present data on the state of maturity of the Organic Matter in the region (Askri *et al.,* 1995). As shown in figure 1b and 1c, dry gas and gas are mainly reached for the Silurian and the Frasnian series. These levels are considered as the best potential source rocks (black shales or hot radioactive shales with graptolites) (Logan and Duddy, 1998; Drid *et al.,* 1998; Kadi *et al.,* 2013; Nedjari and Ait Ouali, 2018). Since a few decades, oil and gas companies worldwide emphasize the advantage to use non-conventional energetic resources to supply the increasing needs we are facing today. In the Timimoun-Ahnet and Adrar regions in particular, the hydrocarbon systems are perfect targets for such mitigations and prospecting (shale gas) (Kaced *et al.,* 2013).

In this work, a well logging analysis was firstly carried out in the Timimoun basin. The resulting data were considered to provide the software TherMO'S developed by Amir (2002) with a database for basin modeling in the region. The figure 2a displays the studied area with the location of the boreholes in the context of the tectonics and information collected in papers such as the thermal gradients recorded in past studies (Lefranc and Conrad, 1974; Beghoul, 1991; Ouali *et al.,* 2007). A lithologic log is shown in figure 2b for Gara El Kahla nearby Timimoun (Nedjari and Ait Ouali, 2018).

Petrophysical and thermal properties are classically estimated to assess (1) the hydrocarbon potential for source rocks, (2) the oil and gas migration from the source rocks and (3) the reservoir's properties for exploration. The thermal cracking of the sedimentary organic matter is controlled by the heating of the source rocks. In fact, hydrocarbon mitigation for exploration should include the rate that a process takes place during the burial history of the basin (burial rates, porosity decrease, thermal gradients variation, heating of the source rocks,...). In particular, the compaction has an effect on the hydrocarbon generation and expulsion processes all through the history of a basin. For the case of the Timimoun-Ahnet basin, it has been suggested from a geochemical approach that the source rocks series might have been under-compacted (Kadi *et al.,* 2013; Nedjari and Ait Ouali, 2018). The authors proposed that it would have then prevented the hydrocarbon liquid from the Silurian from any expulsion processes, and consequently favored a higher state of maturity.

Here, the purpose of the presented study, is to contribute to a better understanding of the hydrocarbon system in a multidisciplinary approach at the geological scale in the Timimoun - Ahnet region. To this aim, the next section presents the materials and methods (well logging analysis and basin modeling) used. Then, the results are described for the source rocks levels (Silurian and Frasnian) and the reservoirs (Upper Devonian - Carboniferous:

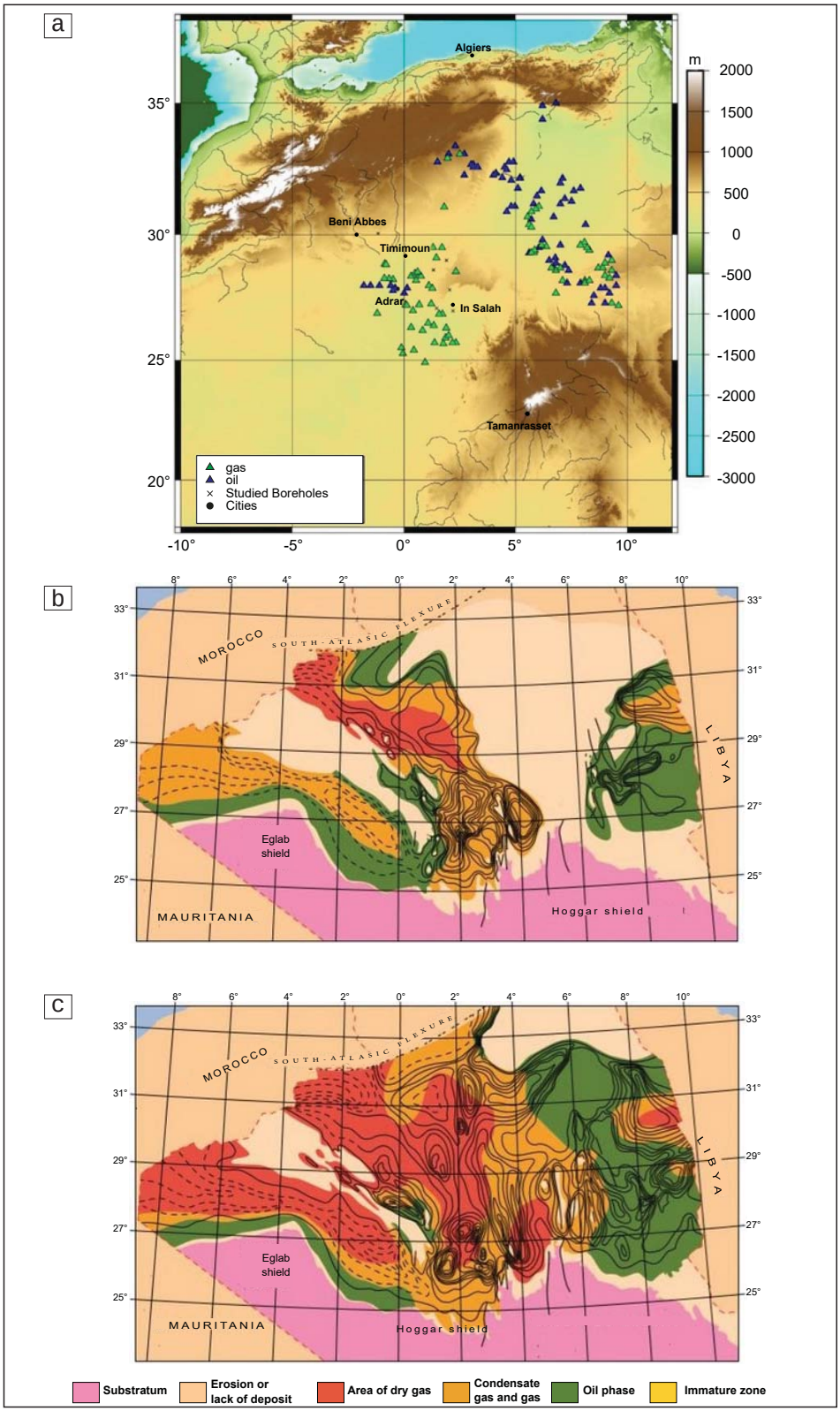

Fig. 1 - (a) Oil and gas resources in Algeria (Askri *et al.*, 1995) (topography : ETOPO 1' from Amante and Eakins (2009)); **(b)** and **(c)** Organic Matter Maturity for the Silurian and Frasnian respectively (Askri *et al.*, 1995).

(a) Ressources en huile et gaz en Algérie (Askri et al., 1995) (topographie: ETOPO 1' (Amante et Eakins (2009)); (b) et (c) Maturité organique du Silurien et du Frasnien, respectivement (Askri et al., 1995).

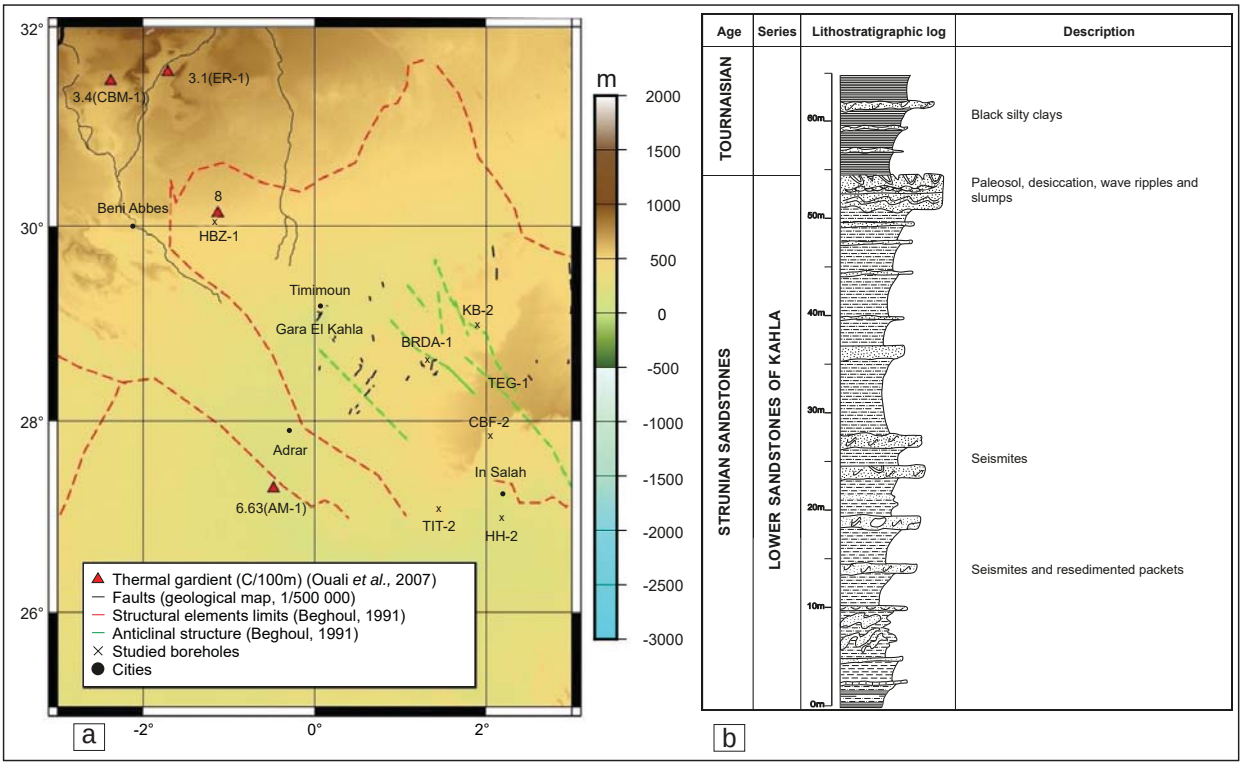

Fig. 2 - (a) Studied area with the location of the 7 boreholes. Tectonic after Beghoul (1991) and geological map of Timimoun: Scale 1/500 000 (Lefranc and Conrad, 1974); Thermal gradients after Ouali *et al.* (2007) for HBZ-1 and AM-1 boreholes. **(b)** Lithostratigraphic log for the Timimoun region for the Strunian and Tournaisian (Nedjari and Ait Ouali, 2018).

(a) Zone étudiée avec localisation des 7 sondages. Tectonique d'après Beghoul (1991) et la carte géologique de Timimoun: échelle 1/500 000 (Lefranc et Conrad, 1974). Gradients thermiques d'après Ouali et al. (2007) pour les sondages HBZ-1 et AM-1. (b) Log lithostratigraphique de la région de Timimoun (Gara El Kahla) (Strunien et Tournaisien) (Nedjari et Ait Ouali, 2018).

Strunian and Tournaisian). The discussion that follows, highlights to what extent the spatio-temporal variation of the petrophysical and thermal parameters computed with basin modeling are explained considering the geodynamic and the tectonic framework. Moreover, the choice to use non-conventional resources in the Timimoun-Ahnet basin is well discussed in regards to all data and information here collected for a global analysis.

II - MATERIALS AND METHODS

II. 1- Well logging analysis

II. 1.1- The lithostratigraphic analysis

Lithology can be evaluated from the gamma ray data. The volume shale is estimated from the following formula (1) (Serra and Serra, 2004a, 2004b):

$$V_{shx} = \frac{GR_x - GR_{clean}}{GR_{shale} - GR_{clean}} \quad (1),$$

where: V_{shx} represents the shale volume for a point X selected in the gamma ray logs, GR_x represents the gamma ray measurements for point X, GR_{shale} corresponds to the gamma ray values for a shale referenced unit (shale base line) and GR_{clean} corresponds either to a clean sand line base or a clean limestone identified as a reference for the selected unit.

II. 1.2- The lithostatic coefficient and the surface porosity for the Timimoun shale

The reconstruction of a basin history relies on the geological units' deposits and consequently on the classical empirical porosity to depth law (Allen and Allen, 1990). During its burial, a geological unit is subjected to compaction induced by the overlying deposits. Then, porosities decrease and fluids are expelled. Parameters that control the burial process in a basin are constrained by intrinsic properties that are the initial porosity and the lithostatic coefficient (Medina and Rimi, 1992).

Here, we used the method developed by Medina and Rimi (1992) to estimate the initial porosity and the lithostatic coefficient for the Timimoun hot shales. The porosity to depth relationship was established using the sonic logs (Oubacha and Belkacem, 2010). Porosity values are firstly deduced from the time-transit values for several points for all the seven boreholes and calculated using the Willy equation (2):

$$\phi = \frac{(\Delta t - \Delta t_{ma})}{(\Delta t - \Delta t_{ma})} \quad (2),$$

where: ϕ is the porosity, Δt is the transit time read on the sonic log, Δt_{ma} is the transit time in the matrix and Δt_f is the transit time in the fluids. For the Timimoun basin, we considered that Δt_{ma} was 54 µs/ft and Δt_f was 189 µs/ft (Bentellis, personal communication, 2010).

The calculations are then plotted in a graph representing the porosity versus the depth and a correlation between all reported values resulted in a law adapted for the considered shale in the basin. The initial porosity and the lithostatic coefficient can then be deduced from the newly established relationship. Conventional empirical laws were as well reported for comparison with the values estimated for the Timimoun shales.

II. 2- Basin Modeling

During the subsidence of a basin, sedimentary sequences are subjected to increasing pressure-temperature conditions. In basin modeling, codes are classically based on the assumption of a constant thermal gradient. The TherMO'S software includes the variation of the thermal gradients and conductivities related to the burial of each stratigraphic sequences (Amir, 2002; Amir *et al.,* 2005, 2008). That feature leads to a better understanding of the timing of hydrocarbons generation through the computing of the thermal energies provided for the sedimentary organic matter cracking during the basin burial history (Amir, 2002). In this work, we only investigate the role of the compaction (backstripping) on the petrophysical and thermal properties that give an insight into the hydrocarbon system in the region.

The flow chart of the TherMO'S software is shown in figure 3. It indicates the input data for all the procedures that estimate the burial and related petrophysical and thermal data. A detailed explanation on the development of the model was presented in previous published papers by Amir *et al.* (2005, 2008).

The stratigraphic database comes from the well logging analysis (lithology, surface porosity, lithostatic coefficient). Then, all petrophysical parameters relatively to the burial history (paleoporosities, thermal paleoconductivities) are injected to estimate the thermal paleogradients, the paleotemperatures and the thermal energies for thermal cracking of the organic matter. The heating of the Sedimentary Organic Matter (SOM) is related to the basal heat flux provided to the sedimentary units and the thickness of each unit. Here, we considered heat flow maps established by Ouali *et al.* (2007) for Algeria.

To simulate the thermal properties (temperatures,...), surface paleotemperatures were included in the model. Deposits and precipitation of calcium carbonates or biogenic apatite

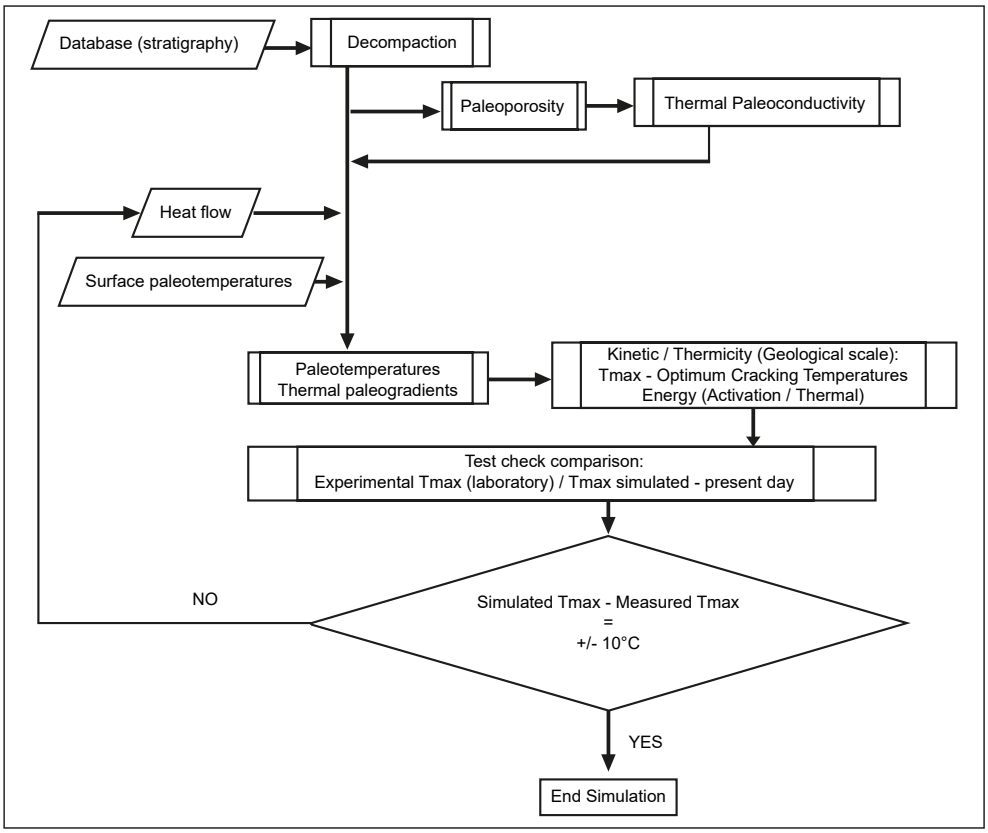

Fig. 3 - Flow chart of the TherMO'S Model (Amir, 2002; Amir *et al.,* 2005, 2008).
Organigramme du modèle TherMO'S (Amir, 2002 ; Amir et al., 2005, 2008).

contain climatic information. Here, data were compiled and calculated using a geochemical approach based on oxygen isotopes contained in phosphates of fossil fish (Kolodny and Luz, 1991). Equations (3) and (4) (Longinelli and Nuti, 1973a; Puceat *et al.,* 2010) permitted to propose surface paleotemperatures for locations that corresponded to the paleogeography of the Saharan Domain (Northern Gondwana) from the Cambrian to present-day:

$$t\ (°C) = 111.4 - 4.3\ (\delta^{18}O_p - \delta^{18}O_w) \quad (3)$$

$$t\ (°C) = 118.7\ (\pm 4.9) - 4.22\ (\pm 0.20)(\delta^{18}O_p - \delta^{18}O_w) \quad (4),$$

where: $\delta^{18}O_p$ represents the oxygen isotope ratio in phosphate and $\delta^{18}O_w$ the oxygen isotopic composition of the surrounding water.

The last data needed to calibrate the simulations are the optimum organic matter thermal cracking temperatures. Here, we considered the Tmax values reported in Kadi *et al.* (2013) for the Silurian and the Frasnian source rocks. We also considered the geochemical analysis from Drid *et al.* (1998) and Lüning *et al.* (2000, 2004) indicating that the source rocks were marked by Organic Matter (OM) with kerogen of type II (Drid *et al.,* 1998; Lüning *et al.,* 2000, 2004).

III - RESULTS

III. 1 - Porosity to depth relationship and lithology from the well logging analysis

The figure 4a and 4b shows the results obtained after we examined the well logging records for the seven boreholes. The sonic logs helped to establish a porosity to depth law (fig. 4a) and the lithology was deduced from the gamma ray data (fig. 4b).

The Sclater and Christie's law here plotted in figure 4a is an empirical relationship widely used as a reference in basin modeling (Sclater and Christie, 1980). The resulting porosity to depth law for the Timimoun shales is detailed in the equation (5) hereby:

$$z = - 1.957 \ln \phi + 8.0605 \quad (5),$$

where: z is the depth and ϕ is the porosity.

The initial porosity equals to 60 % and the lithostatic coefficient "c" is 0.51. The results show that the lithostatic coefficient is the same that the one estimated by Sclater and Christie (1980) (fig. 4a). As for the initial porosity, the calculated value is closed to those from Sclater and Christie (1980) and Medina and Rimi (1992).

Finally, our results show three main porosity clusters. One group characterizes the Frasnian (Upper Devonian), the Tournaisian and the Visean (Carboniferous) units. The estimated values are low in comparison with the Sclater and Christie's law. A second group is defined for the Eifelian (Middle Devonian) and the Famennian (Upper Devonian) series. The corresponding values are closed to the Sclater and Christie's law. A third group highlights the Silurian and the Lochkovian (Lower Devonian) series. The estimated values are high when compared with the Sclater and Christie's law.

In regards to the discrepancy highlighted between these results and the Sclater and Christie's law (1980), the lithology deduced from the gamma ray data is here reported for the source rocks (Silurian, Frasnian) and the reservoirs from the Upper Devonian - Carboniferous (Strunian, Tournaisian) series only (fig. 4b). While the Silurian series are totally shaly for all the considered boreholes, we can observe that for the Frasnian, the limestone and the shale content vary in the studied area (fig. 4b, left). As for the reservoirs, we notice that the Strunian series have a sandy content higher than the Tournaisian series (fig. 4b, right). The Tournaisian deposits are mainly shaly despite a low sand content.

III.2- Burial history for the source rocks (Silurian, Frasnian) and the reservoirs (Strunian, Tournaisian)

The results here presented show the burial history for the source rocks' levels (Silurian and the Frasnian "hot shale") and the reservoirs (Strunian, Tournaisian) simulated with the Ther-MO'S software for the seven studied boreholes (figs. 5 and 6). In addition, the compilation of the geodynamic setting is displayed with the results obtained from the modeling for a global regional understanding of the burial processes at the geological time.

Three main burial phases are identified for both series for the source rocks (fig. 5). Relatively to these successive phases, three episodes that record the acceleration of the burial are defined. These correspond to the Siluro-Devonian Phase "SDP" (between 407-397 Ma), the Devonian - Carboniferous Phase "DCP" (between 375-357 Ma) and the Paleo-Mesozoic Phase "PMP" (between 145-96 Ma) (fig. 5). For each of these episodes, the burial rates are calculated and reported for the seven boreholes (tables as inset for each figure). The results obtained indicate that, in particular, the DCP is marked by the highest burial rates for all the seven boreholes for both source rocks' series (fig. 5a and 5b). We noted as well that the CaV, which is correlated with the Hercynian Compressive Motion (Visean), recorded the highest burial rates for the reservoirs (Strunian, Tournaisian). Discrepancy for the values is observed according to the location of the boreholes. During the DCP, the highest values were found for TIT-2 (Silurian deposits: 65.5 m/Ma; Frasnian deposits: 81.6 m/Ma), TEG-1 (Silurian deposits: 57.9 m/Ma; Frasnian deposits: 75.4 m/Ma) and HBZ-1 (Silurian deposits: 49 m/Ma; Frasnian deposits: 66.1 m/Ma) (fig. 5a and 5b).

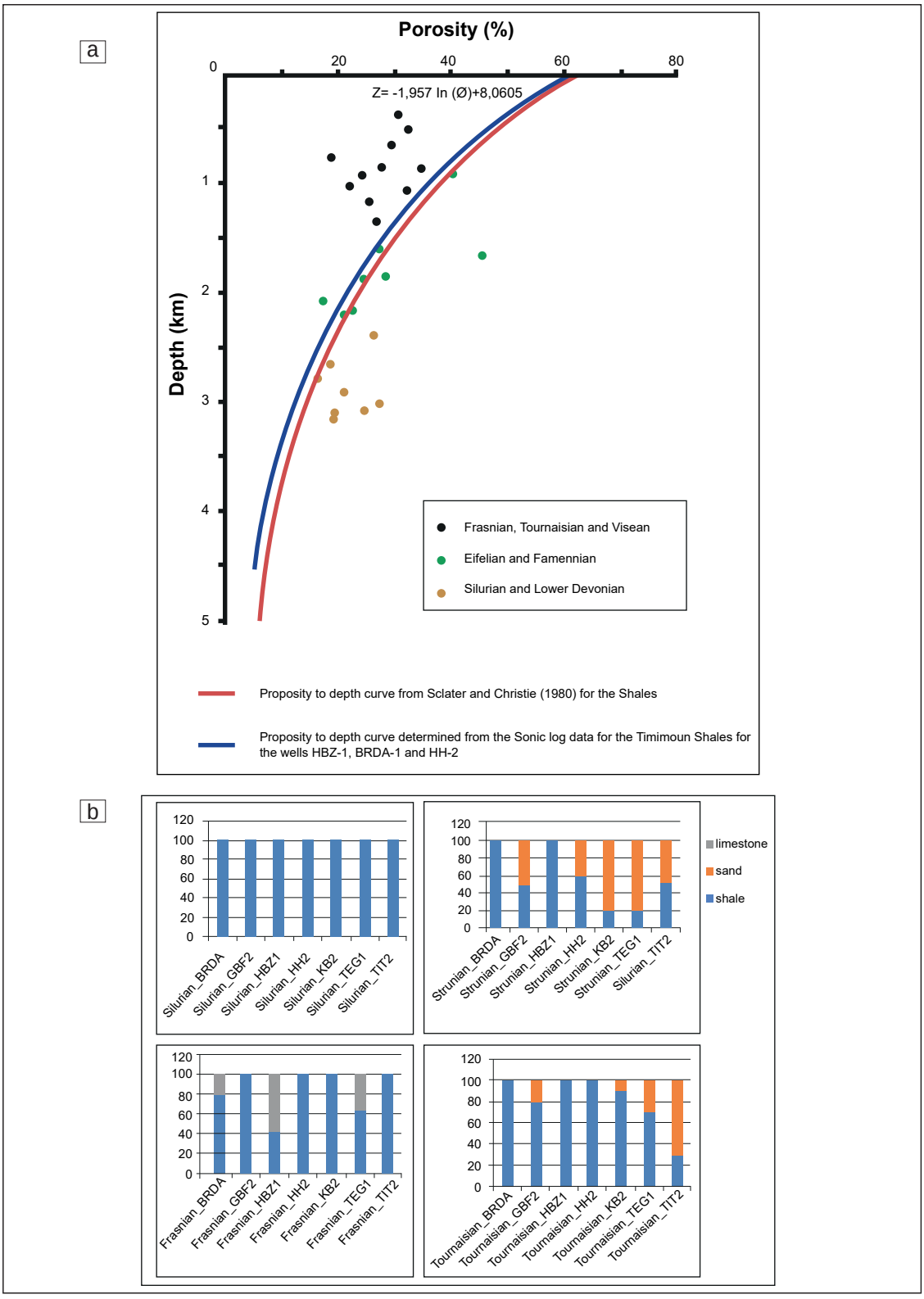

Fig. 4 - Well logging analysis results. **(a)** Porosity to depth law for the shales of Timimoun basin from sonic logs; **(b)** Lithology deduced from gamma ray logs for the source rocks levels (left: Silurian, Frasnian) and the reservoirs (right: Strunian, Tournaisian).

Résultats d'analyse diagraphique. (a) Loi porosité-profondeur pour les argiles du bassin de Timimoun à partir des logs sonic; (b) Lithologie déduite des logs gamma ray pour les niveaux de roches mères (gauche : Silurien, Frasnien) et réservoirs (droite : Strunien, Tournaisien).

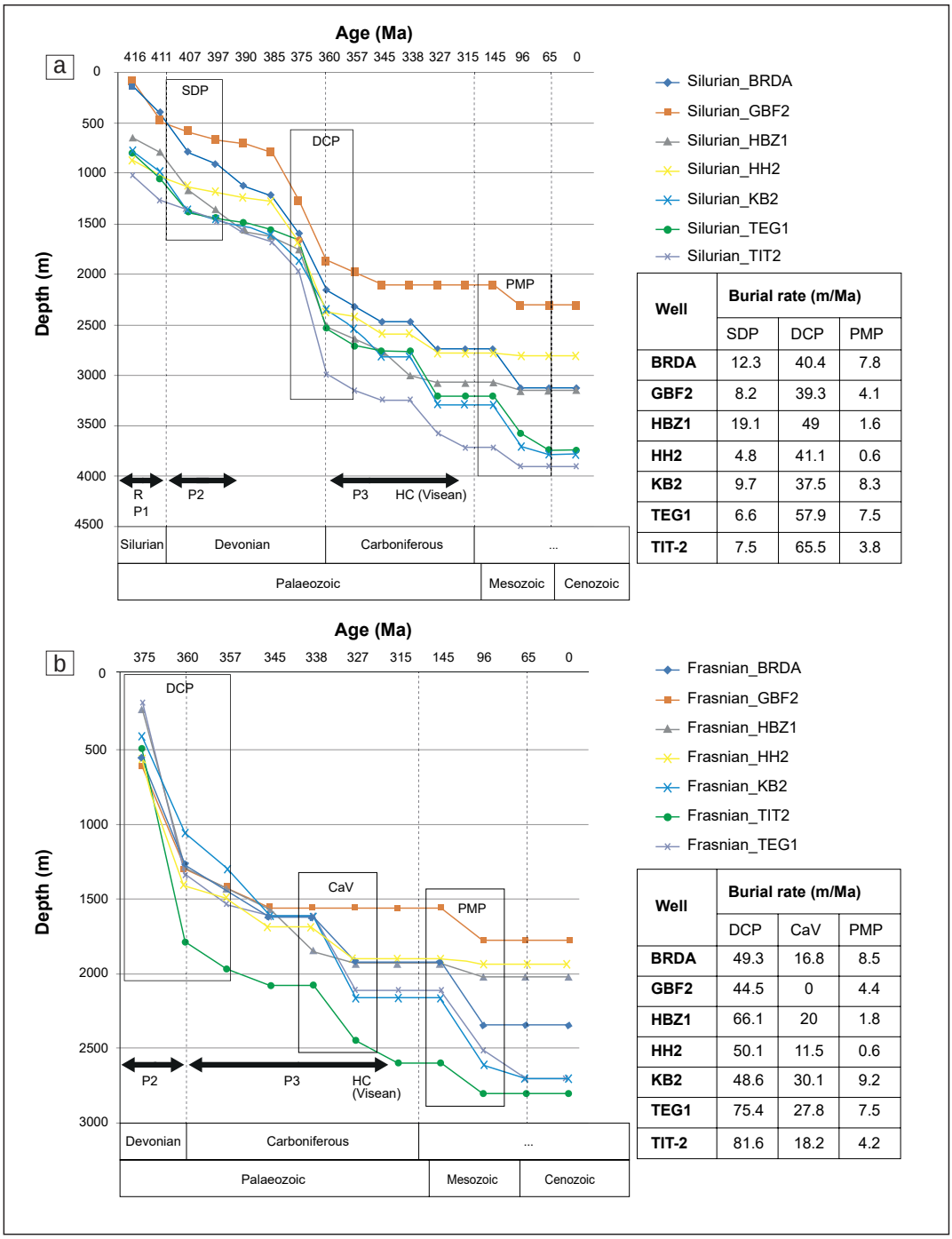

Well	Burial rate (m/Ma)		
	SDP	DCP	PMP
BRDA	12.3	40.4	7.8
GBF2	8.2	39.3	4.1
HBZ1	19.1	49	1.6
HH2	4.8	41.1	0.6
KB2	9.7	37.5	8.3
TEG1	6.6	57.9	7.5
TIT-2	7.5	65.5	3.8

Well	Burial rate (m/Ma)		
	DCP	CaV	PMP
BRDA	49.3	16.8	8.5
GBF2	44.5	0	4.4
HBZ1	66.1	20	1.8
HH2	50.1	11.5	0.6
KB2	48.6	30.1	9.2
TEG1	75.4	27.8	7.5
TIT-2	81.6	18.2	4.2

Fig. 5 - Burial curves for the Silurian **(a)** and Frasnian **(b)** boreholes. Geodynamic events (after Drid, 1989; Nedjari and Ait Ouali, 2018): P1: Taconic Compression Phase; R: Distension Phase; P2: Ardennaise Phase (Caledonian); P3: Tectonic/Thermal Subsidence; HC: Early Hercynian Compression (Visean). Inset: Tables of burial rates estimated for specific phases: SDP: Siluro-Devonian (407-397 Ma); DCP: Devonian Carboniferous (375-347 Ma); CaV: Carboniferous Visean (345-327 Ma); PMP: Paleo-Mesozoic (145-96 Ma).

Courbes d'enfouissement pour les sondages du Silurien (a) et du Frasnien (b). Evènements géodynamiques (d'après Drid et al., 1989; Nedjari et Ait Ouali, 2018): P1: Phase taconique compressive; R: Phase de distension; P2: Phase ardennaise (Calédonien); P3: Subsidence tectonique/thermique; HC: Compression hercynienne précoce (Viséen).

Encart: Tables des vitesses d'enfouissement estimées pour des phases spécifiques: SDP: Siluro-Dévonien (407-397 Ma); DCP: Dévonien-Carbonifère (375-347 Ma); CaV: Carbonifère-Viséen (345-327 Ma); PMP: Paléo-Mésozoïque (145-96 Ma).

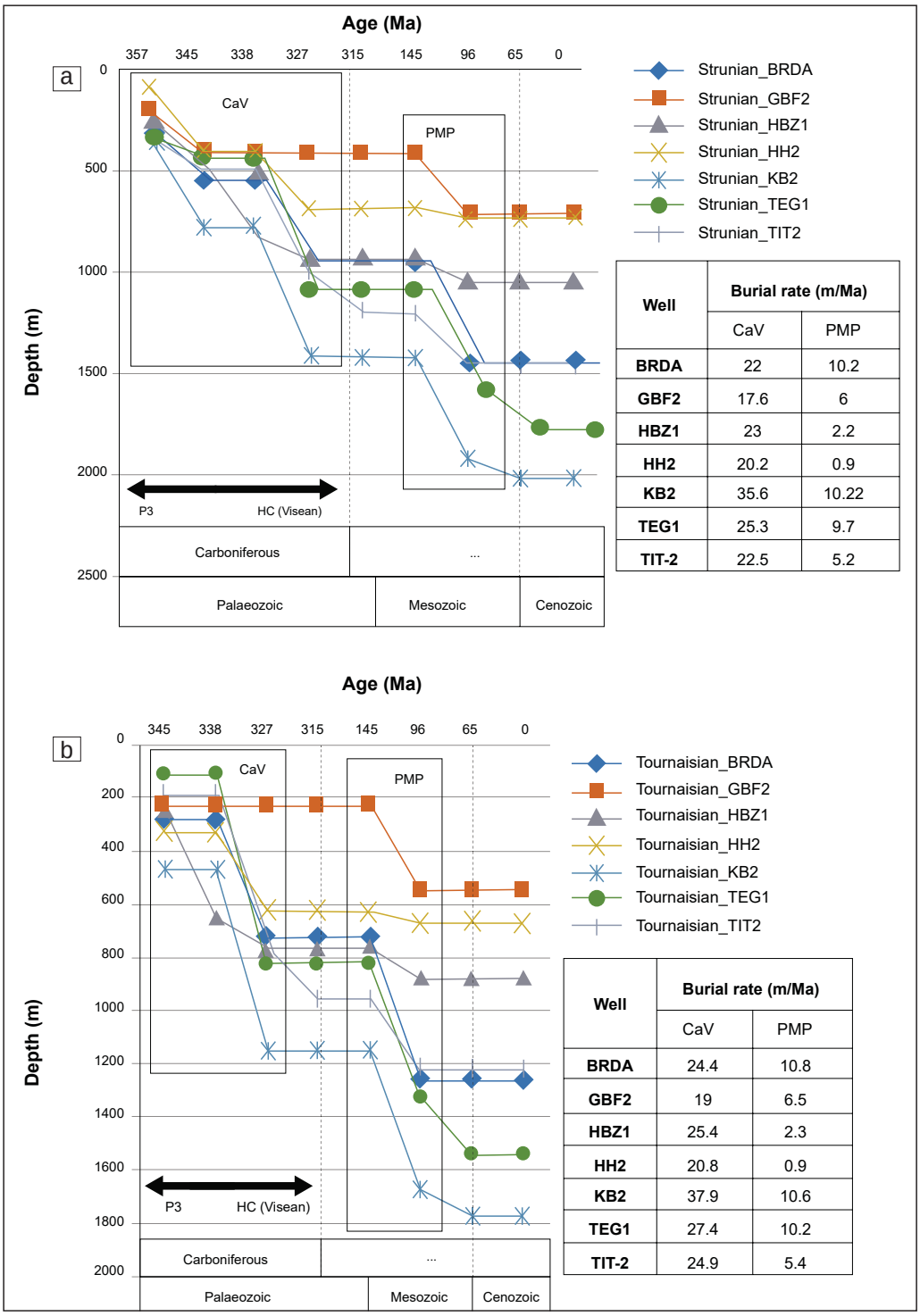

Well	Burial rate (m/Ma)	
	CaV	PMP
BRDA	22	10.2
GBF2	17.6	6
HBZ1	23	2.2
HH2	20.2	0.9
KB2	35.6	10.22
TEG1	25.3	9.7
TIT-2	22.5	5.2

Well	Burial rate (m/Ma)	
	CaV	PMP
BRDA	24.4	10.8
GBF2	19	6.5
HBZ1	25.4	2.3
HH2	20.8	0.9
KB2	37.9	10.6
TEG1	27.4	10.2
TIT-2	24.9	5.4

Fig. 6 - Burial curves for the reservoirs of Strunian **(a)** and Tournaisian **(b)** for the seven boreholes. Geodynamic events (after Drid, 1989; Nedjari and Ait Ouali, 2018): P3: Tectonic/Thermal Subsidence; HC: Early Hercynian Compression.
Inset: Tables of burial rates estimated for specific phases: CaV: Carboniferous Visean (345-327 Ma); PMP: Paleo-Mesozoic (145-96 Ma).

Courbes d'enfouissement pour les niveaux réservoirs du Strunien (a) et du Tournaisien (b) pour les sept sondages. Evènements géodynamiques (d'après Drid et al., 1989; Nedjari et Ait Ouali, 2018): P3: Subsidence tectonique/thermique; HC: Compression hercynienne précoce (Viséen).
Encart: Tables des vitesses d'enfouissement estimées pour les phases spécifiques: CaV: Carbonifère-Viséen (345-327 Ma); PMP: Paléo-Mésozoïque (145-96 Ma).

Despite the values obtained during the CaV phase for the reservoirs (Strunian, Tournaisian) showing less discrepancy, we noted that the highest values were estimated for KB2 (Strunian deposits: 35.6 m/Ma; Tournaisian deposits: 37.9 m/Ma), TEG1 (Strunian deposits: 25.3 m/Ma; Tournaisian deposits: 27.4 m/Ma) and HBZ1 (Strunian deposits: 23 m/Ma; Tournaisian deposits: 25.4 m/Ma).

III.3- Simulation of the petrophysical and thermal properties

Figures 7 and 8 report the simulation of the porosities for the source rocks and the reservoirs respectively. Here, we observe the three main phases and episodes that resulted from the burial analysis for the source rocks and the reservoirs.

For the Silurian series (fig. 7a), the highest decrease has been evidenced for the DCP. In particular, the highest values are found for TEG1(0.7%/Ma), TIT-2 (0.7%/Ma), HH2 (0.56% /Ma) and HBZ1 (0.53 %/Ma). GBF2 is marked by the lowest decrease (0.005%/Ma). For the Frasnian series, the porosities simulated are higher than those obtained for the Silurian series. The values calculated at present time range between 16% to 28% (fig. 7b). Here again, the highest decrease of the porosity is observed for TEG1 (1.83 %/Ma), HBZ1(1.75% /Ma) and TIT2 (1.66 %/Ma).

Finally, at present time, we found porosities between 20% to 7% for the Silurian series (fig. 7a). Data published by several authors helped to validate these computations. Askri *et al.* (1995) indicated that to the NE and SW of the Timimoun basin, porosities of 15% to 20% were observed while in the center, the porosity values usually fall between 7% to 12%.

For the Strunian series, the lowest porosities values are obtained for TEG1 and KB2 (under 30%) (fig. 8a). Currently, porosity values under 35% are obtained for TIT2, BRDA. For the Tournaisian series, we note that the highest decrease of the porosity is simulated during the CaV for KB-2 (fig. 8b).

Finally, the mean thermal gradients calculated for HBZ-1 are as well reported in figure 8 (tables as inset) for distinct ages for the Strunian and the Tournaisian. The values range between 7.5°C/100m to 6°C/100m. These results are in good agreement with the data published by Ouali *et al.* (2007) and reported in figure 2a (8°C/100m). It clearly shows that the region is subjected to an abnormal higher thermicity unlike the rest of the country where according to Ouali *et al.* (2007), the mean thermal gradient is closed to 4°/100m.

From 375-357 Ma (Upper Devonian-Carboniferous), the thermal energies provided to the Silurian deposits are all above 50 kcal/mol (fig. 9, tables as inset). For the Frasnian deposits, the energies are lower. The highest values are obtained for TIT2, TEG1 and HBZ-1. From 345 to 327 Ma (Carboniferous), TEG1, TIT2 and HBZ1 are the locations where the highest thermal energies are found for both the Silurian and the Frasnian series. The energies provided to the Silurian deposits all reached above 60 kcal/mol.

Finally, the evolution of the thermal gradients with time for the source rocks deposits is shown in figure 9. We observe the three main phases and episodes that resulted from the burial analysis for the seven boreholes (fig. 9). The thermal gradients vary from 82 to 45 °C/km. Our findings and results are supported by previous investigations. Geochemical analysis revealed that the current geothermal gradients are relatively low in the Ahnet basin at present time (34°C-45°C /km) when compared with paleogeothermal gradients (60-70°C/km) (Logan and Duddy, 1998).

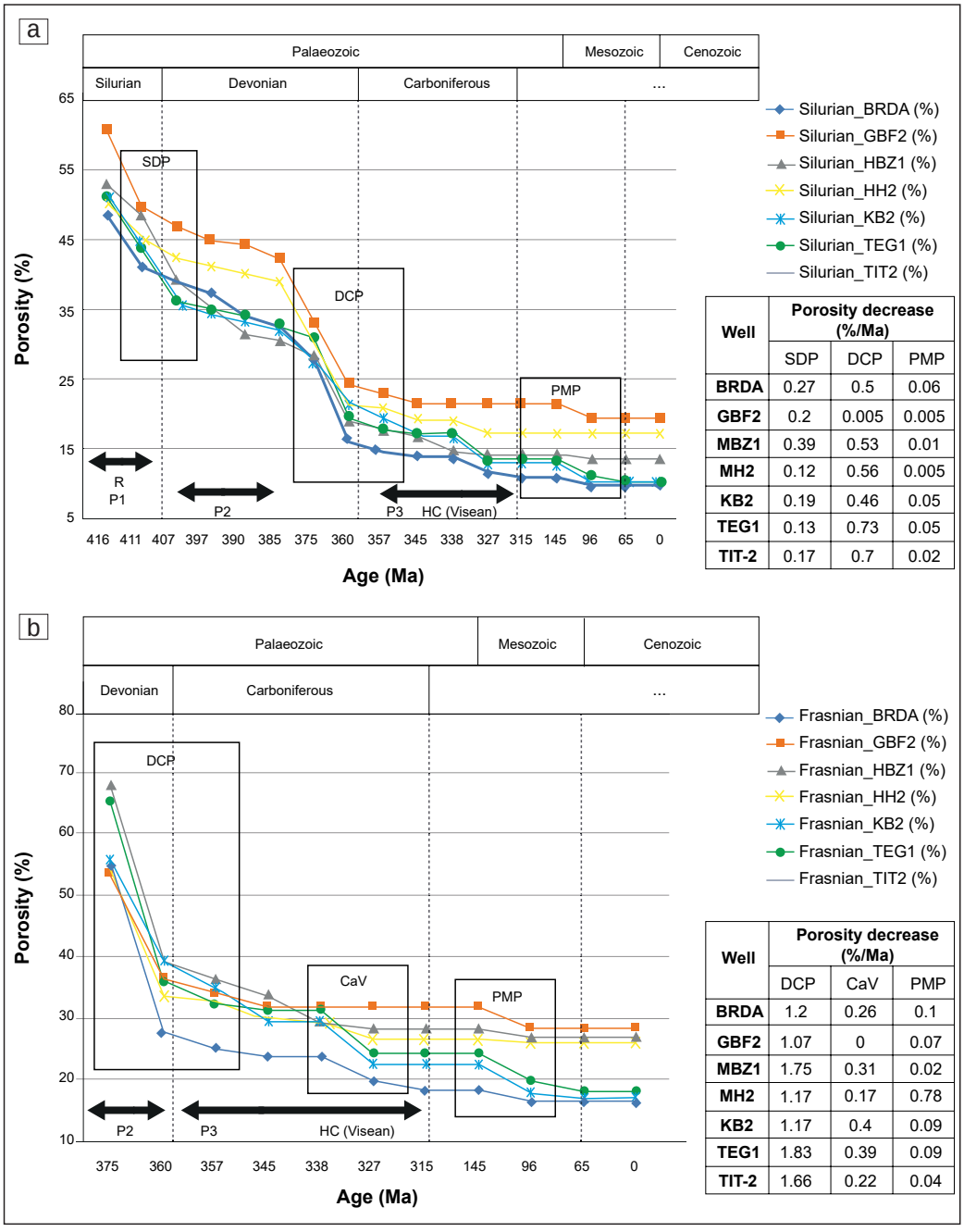

Well	Porosity decrease (%/Ma)		
	SDP	DCP	PMP
BRDA	0.27	0.5	0.06
GBF2	0.2	0.005	0.005
MBZ1	0.39	0.53	0.01
MH2	0.12	0.56	0.005
KB2	0.19	0.46	0.05
TEG1	0.13	0.73	0.05
TIT-2	0.17	0.7	0.02

Well	Porosity decrease (%/Ma)		
	DCP	CaV	PMP
BRDA	1.2	0.26	0.1
GBF2	1.07	0	0.07
MBZ1	1.75	0.31	0.02
MH2	1.17	0.17	0.78
KB2	1.17	0.4	0.09
TEG1	1.83	0.39	0.09
TIT-2	1.66	0.22	0.04

Fig. 7- Porosity curves for Silurian **(a)** and Frasnian **(b)** series for the seven boreholes. Geodynamic events (after Drid, 1989; Nedjari and Ait Ouali, 2018): P1: Taconic Compression Phase; R: Distension Phase; P2: Ardennaise Phase (Caledonian); P3: Tectonic/Thermal Subsidence; HC: Early Hercynian Compression.

Inset: Tables of the rate of porosity decrease for specific phases: SDP: Siluro- Devonian (407-397 Ma); DCP: Devonian Carboniferous (375-347 Ma); CaV: Carboniferous-Visean (345-327 Ma); PMP: Paleo-Mesozoic (145-96 Ma).

Courbes de porosité des séries du Silurien (a) et Frasnien (b) pour les sept sondages. Evènements géodynamiques (d'après Drid, 1989; Nedjari et Ait Ouali, 2018): P1: Phase taconique compressive; R: Phase de distension; P2: Phase ardennaise (Calédonien); P3: Subsidence tectonique/thermique; HC: Compression hercynienne précoce (345-327 Ma).

Encart: Tables de diminution de la porosité pour les phases spécifiques: SDP: Phase du Siluro-Dévonien (407-397 Ma); DCP: Phase du Dévonien-Carbonifère (375-347 Ma); CaV: Carbonifère-Viséen (345-327 Ma); PMP: Phase du Paléo-Mésozoïque (145-96 Ma).

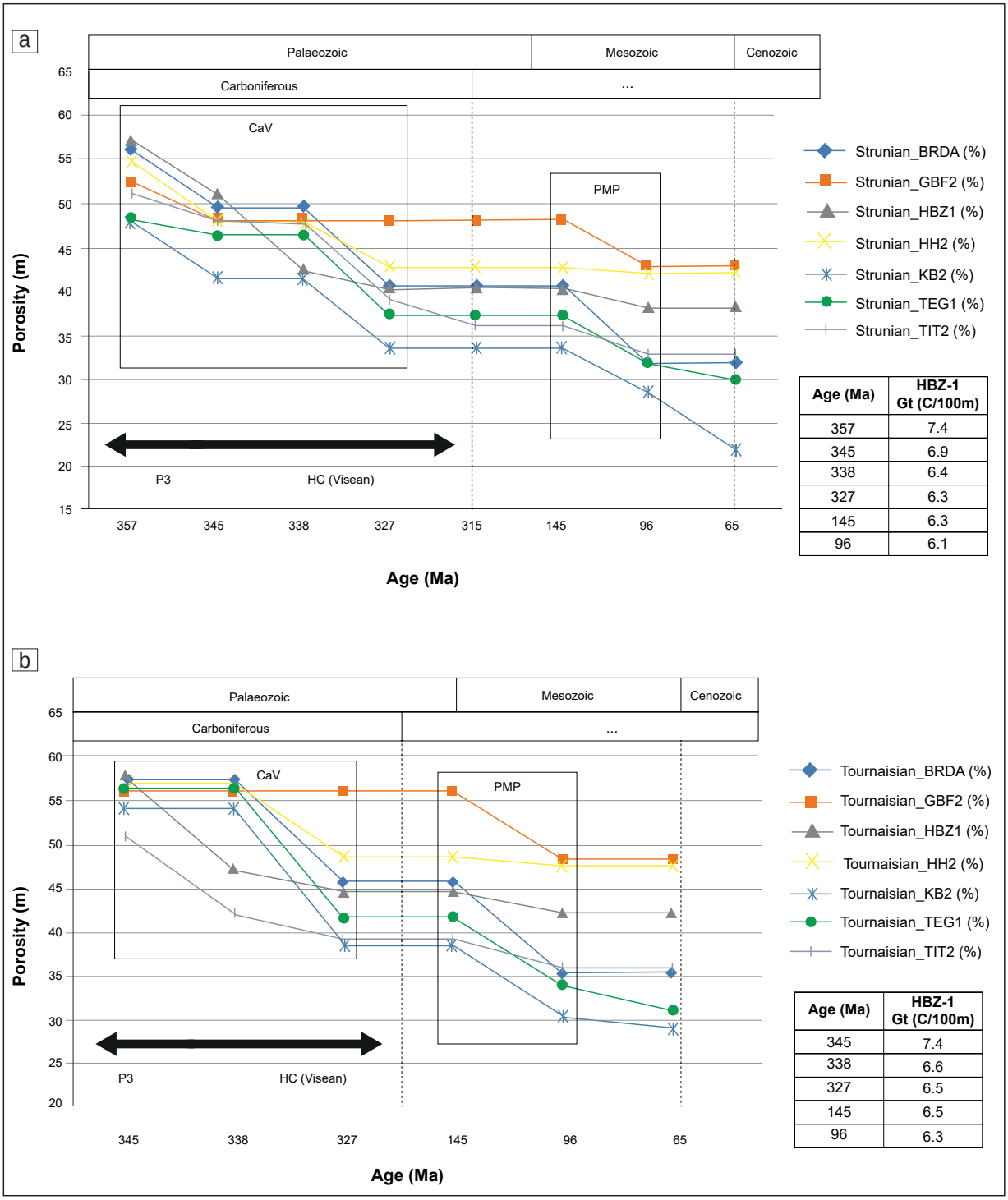

Age (Ma)	HBZ-1 Gt (C/100m)
357	7.4
345	6.9
338	6.4
327	6.3
145	6.3
96	6.1

Age (Ma)	HBZ-1 Gt (C/100m)
345	7.4
338	6.6
327	6.5
145	6.5
96	6.3

Fig. 8 - Porosity curves for the Strunian **(a)** and Tournaisian **(b)** reservoirs for the seven boreholes. Geodynamic events (after Drid, 1989; Nedjari and Ait Ouali, 2018); P3: Tectonic/Thermal Subsidence; HC: Early Hercynian Compression. CaV: Carboniferous Visean (345-327 Ma); PMP: Paleo-Mesozoic (145-96 Ma). Inset: Tables of thermal gradients estimated for HBZ-1 (°C/100m) for specific geological time.

Courbes de porosité pour les réservoirs du Strunien (a) et Tournaisien (b) pour les sept sondages. Evènements géodynamiques (d'après Drid, 1989; Nedjari et Ait Ouali, 2018); P3: Subsidence tectonique/ thermique; HC: Compression hercynienne précoce; CaV: Carbonifère Viséen (345-327 Ma); PMP: Paléo-Mésozoïque (145-96 Ma).

Encart: Tables des gradients thermiques estimés pour HBZ-1 (°C/100m) pour un temps géologique spécifique.

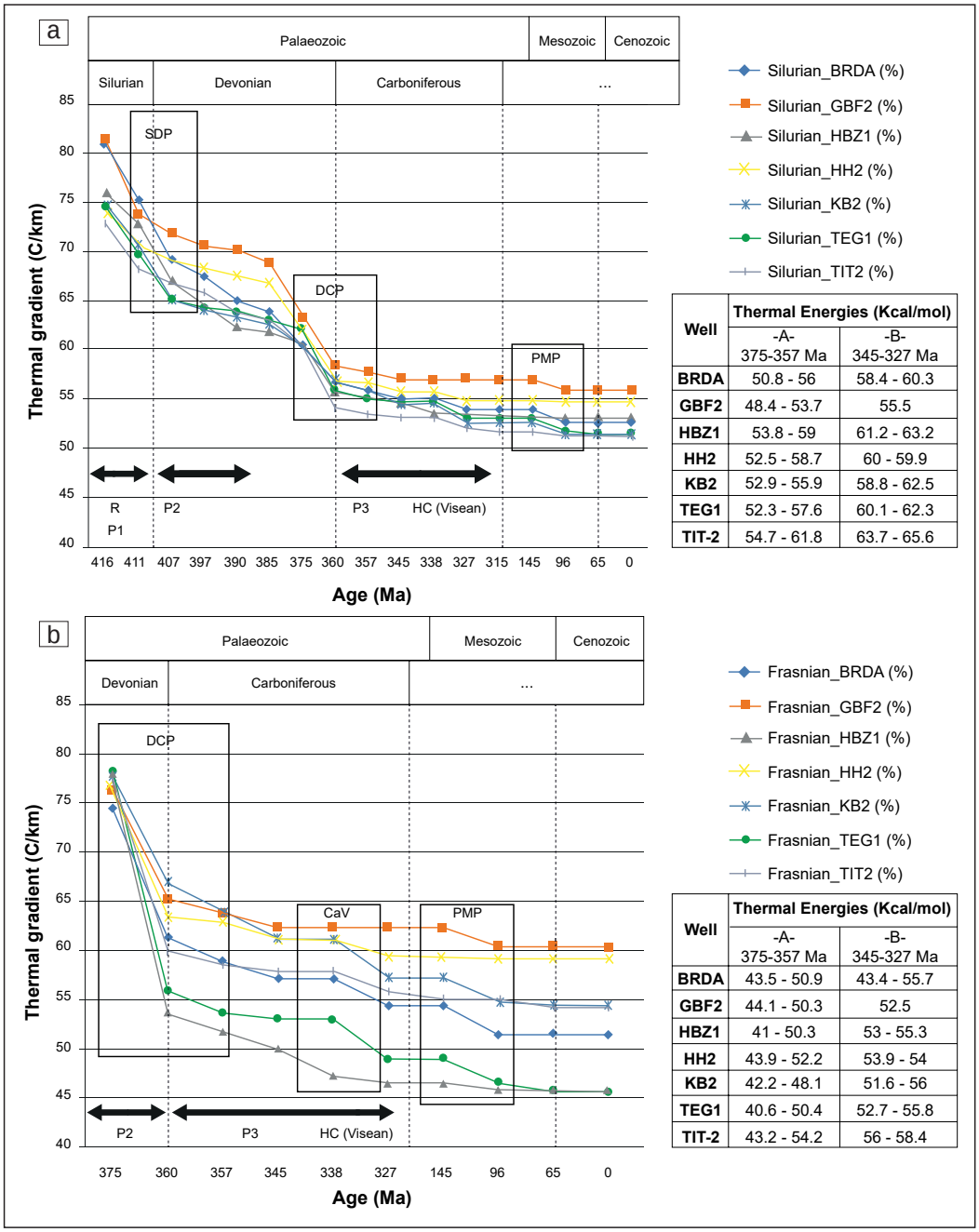

Well	Thermal Energies (Kcal/mol)	
	-A- 375-357 Ma	-B- 345-327 Ma
BRDA	50.8 - 56	58.4 - 60.3
GBF2	48.4 - 53.7	55.5
HBZ1	53.8 - 59	61.2 - 63.2
HH2	52.5 - 58.7	60 - 59.9
KB2	52.9 - 55.9	58.8 - 62.5
TEG1	52.3 - 57.6	60.1 - 62.3
TIT-2	54.7 - 61.8	63.7 - 65.6

Well	Thermal Energies (Kcal/mol)	
	-A- 375-357 Ma	-B- 345-327 Ma
BRDA	43.5 - 50.9	43.4 - 55.7
GBF2	44.1 - 50.3	52.5
HBZ1	41 - 50.3	53 - 55.3
HH2	43.9 - 52.2	53.9 - 54
KB2	42.2 - 48.1	51.6 - 56
TEG1	40.6 - 50.4	52.7 - 55.8
TIT-2	43.2 - 54.2	56 - 58.4

Fig. 9- Thermal gradients for the source rocks of Silurian **(a)** and Frasnian **(b)** for the seven boreholes. Geodynamic Events (From Drid, 1989; Nedjari and Ait Ouali, 2018): P1: Taconic Compression Phase; R: Distension Phase; P2: Ardennaise Phase (Caledonian); P3: Tectonic/Thermal Subsidence; HC: Early Hercynian Compression (Visean). SDP: Siluro-Devonian (407-397 Ma); DCP: Devonian Carboniferous (375-347 Ma); CaV: Carboniferous Visean (345-327 Ma); PMP: Paleo-Mesozoic (145-96 Ma).
Inset: tables:Thermal Energies (kcal/mol) for episodes A (375-357 Ma) and B (345-327 Ma).

Gradients thermiques pour les roches mères du Silurien (a) et du Frasnien (b) pour les sept sondages. Evènements géodynamiques (d'après Drid, 1989; Nedjari et Ait Ouali, 2018): P1: Phase taconique compressive ; R : Phase de distension; P2: Phase ardennaise (Calédonien); P3: Subsidence tectonique/thermique; HC: Compression hercynienne précoce (Viséen); SDP: Siluro-Dévonien (407-397 Ma); DCP: Dévonien-Carbonifère (375-347 Ma) ; CaV: Carbonifère-Viséen (345-327 Ma); PMP: Phase du Paléo-Mésozoïque (145-96 Ma).
Encart: Tables des énergies thermiques (kcal/mol) pour les épisodes A (375-327 Ma) et B (345-327 Ma).

IV - DISCUSSION

In general, the burial rates showed evidences for syn-sedimentary tectonics and geodynamic events that affected the region during the formation and evolution of the basin. Moreover, the three main phases we identified are in line with previous studies that examined the geodynamic evolution of the basin in the region (Nedjari and Ait Ouali, 2018). These studies were supported by field investigations in the region and in the nearby Saharan basins (Nedjari *et al.,* 2009; Nedjari and Ait Ouali, 2018).

From the results obtained, we suggest that a higher thermal regime could be associated to the porosity data estimated from the sonic logs. In fact, the porosity to depth obtained for the group shale of Frasnian-Tournaisian-Visean could be related to a higher thermicity recorded in the Ougarta Range either during the Hercynian or the Upper Triassic. Previous studies related to the Triassic Province in the Saharan Domain revealed that magmas filled reactivated faults (Nedjari *et al.,* 2009). Published microthermometric data indicated that high temperatures paleo-fluids have circulated in fractures and faults in the Sbaa basin (Wazir *et al.,* 2013). Wazir *et al.* (2013) also highlighted that the tectonic activity related to the Hercynian orogeny played a major role in the acidic fluid circulation from the Silurian shale, rich in organic matter and sulfides flowing into the reservoir. Therefore, the sedimentary series in the Timimoun basin probably have been subjected to hydrothermal fluid circulation that could have destroyed the porosities in the Upper Devonian (Frasnian) and in the Carboniferous formations.

According to Logan and Duddy (1998), the high geothermal gradients that resulted from Hercynian and thermal regional events during the Upper Triassic might have consequently induced a very fast heating of the source rocks, beyond the threshold for hydrocarbon generation. The existing liquid hydrocarbons could have been then cracked to gas by that period. In fact, the level of energy necessary for oil cracking for a type II kerogen is between 54-57 kcal/mol (Waples, 1994). According to Drid *et al.* (1998), the Silurian hot shale entered the oil window at the Lower Carboniferous in the Timimoun depression. As for the Ahnet depression, the Silurian source rocks entered in the oil window phase only at the end of the Visean. The Frasnian source rocks entered in the oil window phase by the Upper Visean in the limit of the Timimoun basin. It is only at the Upper Carboniferous that both the Silurian and the Frasnian source rocks entered in the gas window phase (Drid *et al.,*1998). Logan and Duddy (1998) noted that for TEG1, the Silurian and the Devonian source rocks were probably sufficiently mature to have generated oil before the Hercynian event. During the Upper Triassic event, they could have been heated though the gas window and any previously reservoired oil would have been cracked (Logan and Duddy, 1998).

Fault reactivations at this period are to be considered when examining not only the geodynamic context but as well the petrophysical resulting parameters. KB-2, TEG-1, BRDA and GBF2 are located in the Timimoun anticline while HBZ1 is located in the north of Timimoun and TIT2 and HH2 in the south of In Salah (fig. 2a). Regarding the tectonic context with the position of these boreholes in the basin (fig. 2a), the analysis of the variation of the burial rates combined to the geodynamic context provides some insights for how active faults and reactivation of faults may have played during the evolution of the burial process and related petrophysical and thermal parameters with time and space.

Finally, past earthquakes were recorded at the base of the Strunian in Gara El Kahla (nearby Timimoun) (fig. 2b) (Nedjari and Ait Ouali, 2018). Moreover, Nedjari *et al.* (2009) reported that the structure of the Timimoun anticline might have begun during the Strunian. In fact, the study here presented, points out the need to pay a special attention to the risks (induced seismicity, environment) due to the process of

shale gas prospecting in the Timimoun region. The supply for energetic resources in places where a higher thermicity is recorded could be as well provided through widening the resources (geothermal, clean renewable energies). A sustainable environmental policy could be applied for these regions thanks to the climate and the related solar, and wind power potential energetic resources.

V - CONCLUSION

In this paper, we investigated the importance to consider in the hydrocarbon mitigation and exploration the burial rates all through the history of a basin on petrophysical and thermal properties of source rocks and reservoirs levels for the Timimoun-Ahnet basin.

On the whole, we conclude and suggest that the hydrocarbon expulsion here is controlled by the combination of (1) the burial rate of the deposits and (2) the regional and geodynamic context. Our results confirm previous studies that describe the successive burial accelerations phases and thermal events that have influenced the petrophysical properties of the source rocks and reservoirs series and the hydrocarbon generation and expulsion.

Acknowledgements

This research did not receive any specific grants from funding agencies in the public, commercial or not-for-profit sections. We are grateful to Dr. Kadi from the SONATRACH for having provided the well logging data and for his help, guidance and advices. This study was prepared with Pr. R. Ait Ouali (USTHB, FSTGAT, Algiers) who passed away on last May 2019. His humility, constant availability, always welcoming anyone and spending time listening and exchanging, sharing as much as he could his deep knowledge, his kindness and generosity will be deeply missed. This paper is a real tribute for all his engagement as Professor and Researcher. We are grateful to him.

REFERENCES

Allen, P.-A. and Allen, J.-R. 1990. Basin Analysis: Principles and applications. *Blackwell Scientific Publications*, 451 p.

Amante, C. and Eakins, B.-W. 2009. ETOPO 1 Arc-Minute Global Relief Model: Procedures, Data Sources and Analysis. *NOAA Technical Memorandum NESDIS NGDC*-24, 19 p.

Amir, L. 2002. Modélisation thermique appliquée aux bassins sédimentaires et utilisant la géochimie organique: conception du logiciel «TherMO'S» pour la reconstitution de l'histoire thermique du bassin parisien à l'échelle séquentielle. *Thèse de Doctorat*, *Université Henri Poincaré*, Nancy I, France, 161 p.

Amir, L. Martinez, L., Disnar, J.-R., Vi-Gneresse, J.-L., Michels, R., Guil-Locheau, F. and Robin, C. 2005. Effect of the thermal gradient variation through geological time on basin modeling, a case study: The Paris basin. *Tectonophysics*, (400), pp. 227-240.

Amir, L., Martinez, L., Disnar, J.-R., Vi-Gneresse, J.-L., Michels, R., Guil-Locheau, F. and Robin, C. 2008. Implications of spatial and temporal evolution of thermal parameters in basin modeling. *Marine and Petroleum Geology*, (25), pp. 759-766.

Askri, H., Belmecheri, A., Benrabah, B., Boudjema, A., Boumendjel, K., Daoudi, M., Drid, M., Ghalem, T., Docca, A.-M., Ghandriche, H., Ghomari, A., Guellati, N., Khennous, M., Lounici, R., Naili, H., Takherist, D. et Terkmani, M. 1995. Géologie de l'Algérie. Contribution de SONATRACH Division Exploration, Centre de Recherche et Développement

et Division Petroleum Engineering et Développement. *Schlumberger WEC Sonatrach I.* pp. 1-93.

Beghoul, M.-S. 1991. Apport et contribution de l'analyse diagraphique à la connaissance d'un bassin sédimentaire. Application au bassin de Timimoun (Algérie). *Thèse de Doctorat*, *Université de Strasbourg*, France, 277 p.

Drid, M. 1989. Quelques aspects de la diagenèse organique et minérale dans le bassin de Timimoun et le sillon de Sbâa (Sahara central-Algérie). *Thèse de Doctorat*, *Université de Bordeaux III*, France, 239 p.

Drid, M., Guandriche, H. and Arezki, A. 1998. The Gas-Bearing of the Ahnet-Timimoun Basin (Algeria): structural evolution and geochemical evaluation, *in*: Exploration and Production. *International Research gas Conference, Gas Research Institute*, pp. 264-276.

Kaced, M., Rahmani, A. et Arab, M. 2013. Le potentiel Shale Gas en Algérie. *Journées d'étude* "*Tight and shale reservoirs*", 17-18 septembre, Alger, Algérie.

Kadi, B., Ait-Ouali, R. et Zazoun, R. 2013. Comparaison de l'histoire thermique des bassins de Timimoun et de Berkine : impact sur l'évolution des argiles et de la matière organique. *Bull. Serv. Geol. Nat. Algérie*, (24), pp. 243-267.

Kolodny, Y. and Lus, B. 1991. Oxygen isotopes in phosphates of fossil fish-Devonian to recent, stable isotope geochemistry: A tribute to Samuel Epstein, *in*: H.-P. Taylor, Jr J.-R. O' Neil and I.-R. Kaplan. *The Geochemical Society, Special Publication. Geochimical Society, Special Publication*, pp. 105-119.

Lefranc, J.-P., Conrad, J.-C et N.R.S. France, 1974. Carte géologique de Timimoun, (1/500 000). Feuille N.H.-31-SO. *SGA.*

Logan, P. and Duddy, L. 1998. An investigation of the thermal history of the Ahnet and Reggane basins, Central Algeria, and the consequences for hydrocarbon generation and accumulation, *in*: Macgregor D.S., Moddy, R.D.J. and Clark-Lowes, D.D. *Petroleum Geology of North Africa, Geological Society,* London, pp. 131-155.

Longinelli, A. and Nuti, S. 1973. Revised phosphate-water isotopic temperature scale. *Earth Planet. Sci. Lett*., (19), pp. 373-376.

Lüning, S., Craig, J., Loydell, D.-K., Storch, P. and Fitches, B. 2000. Lower Silurian "hot shales" in North Africa and Arabia: regional distribution and depositional model. *Earth-Sci. Rev*. (49), pp. 121-200.

Lüning, S., Wendt, J., Belka, Z. and Kauff-Man, B. 2004. Temporal-spatial reconstruction of the early Frasnian (Late Devonian) anorexia in NW Africa: new field from the Ahnet Basin (Algeria). *Sediment. Geol*. (163), pp. 237-264.

Medina, F. et Rimi, A. 1992. Détermination des coefficients de compaction pour les calcaires et les argilites du bassin côtier mésozoïque marocain. *Bull. Inst. Sci. Rabat*. (16), pp. 60-64.

Nedjari, R. et Ait Ouali, R. 2018. Le Gourara-Timimoun: de la synéclise hercynienne atypique aux continentaux. *Mémoire du Service Géologique de l'Algérie*, (20), pp. 3-49.

Nedjari, A., Ait Ouali, R., Hamdidouche, R., Benhamouche, A., Debaghi, F., Amrouche, F. et Messamri, K. 2009. La géologie saharienne revisitée (1980-2009). *Mém. Serv. Géol. Nat.,* pp. 77-170.

Ouali, S., Khellaf, A. et Baddari, K. 2007. Etude des ressources géothermiques du Sud algérien. *Revue des Energies Renouvelables*, (10), pp. 407-414.

Oubacha, N. et Belkacem, H. 2010. Apport des diagraphies et de la simulation numérique dans l'évaluation des paramètres d'enfouissement des séries du Paléozoïque dans le bassin de Timimoun-Ahnet. *Mémoire de fin d'études Ingénieur*, *USTHB*, 79 p.

Puceat, E., Joachimski, M.-M., Bouilloux, A., Monnat, F., Bonin, A., Motreuil, S., Moriniere, P., Henard, S., Mourin, J., Dera, G. and Quesne, D. 2010. Revised phosphate-water fractionation equation reassessing paleotemperatures derived from biogenic apatite. *Earth Planet. Sci. Lett*. (298), pp. 135-142.

Sclater, J.-G. and Christie, P.-A-F. 1980. Continental Streching: An explanation of the Post-Mid Cretaceous subsidence of the Central North Sea basin. *J. Geophys. Res*. (85), pp. 3711-3739.

Serra, O. and Serra, L. 2004a. Total natural radioactivity measurement, *in* : Well logging Data Acquisition and Applications. Mery-Corbon-France, pp. 221-230.

Serra, O. and Serra, L. 2004b. Spectrometry of natural activity, *in* : Well logging Data Acquisitions and Applications. Serralo, Mery-Corbon-France, pp. 231-252.

Waples, D.-W. 1994. Maturity modeling: thermal modeling: thermal indicators, hydrocarbons generation, and oil cracking, *in*: Magoon, L.-B. and W.-G. Dow. *The Petroleum System from Source to Trap, AAPG Memoir*, pp. 285-306.

Wazir, L., Pagel, M., Tournier, F., Portier, E. and Renac, C. 2013. Role of compressive tectonics on gas charging into the Ordovician sandstone reservoirs in the Sbaâ basin, Algeria, constrained by fluid inclusions and mineralogic data. *Geofluids* (14), pp. 106-126.